Mol Biol Rep (2012) 39:5589–5598
DOI 10.1007/s11033-011-1363-4

Molecular characterization of a KIF3B-like kinesin gene in the testis of *Octopus tankahkeei* (*Cephalopoda, Octopus*)

Ran Dang · Jun-Quan Zhu · Fu-Qing Tan · Wei Wang · Hong Zhou · Wan-Xi Yang

Received: 16 July 2011 / Accepted: 12 December 2011 / Published online: 20 December 2011

Abstract KIF3B is known for maintaining and assembling cilia and flagellum. To date, the function of KIF3B and its relationship with KIF3A during spermiogenesis in the cephalopod *Octopus tankahkeei* remains unknown. In the present study, we characterized a gene encoding a homologue of rat KIF3B in the *O. tankahkeei* testis and examined its temporal and spatial expression pattern during spermiogenesis. The cDNA of KIF3B was obtained with degenerate and RACE PCR and the distribution pattern of *ot-kif3b* were observed with RT-PCR. The morphological development during spermiogenesis was illustrated by histological and transmission electron microscopy and mRNA expression of *ot-kif3b* was observed by in situ hybridization. The 2,365 nucleotides cDNA consisted of a 102 bp 5′ untranslated region (UTR), a 2,208 bp open reading frame (ORF) encoding a protein of 736 amino acids, and a 55 bp 3′ UTR. Multiple alignments revealed that the putative Ot-KIF3B shared 68, 68, 69, 68, and 67% identity with that of *Homo sapiens*, *Mus musculus*, *Gallus gallus*, *Danio rerio*, and *Xenopus laevis*, respectively, along with high identities with Ot-KIF3A in fundamental structures. *Ot-kif3b* transcripts appeared gradually in early spermatids, increased in intermediate spermatids and maximized in drastically remodeled and final spermatids. The *kif3b* gene is identified and its expression pattern is demonstrated for the first time in *O. tankahkeei*. Compared to *ot-kif3a* reported by our laboratory before, our data suggested that the putative heterodimeric motor proteins Ot-KIF3A/B may be involved in intraspermatic transport and might contribute to structural changes during spermiogenesis.

Keywords ot-KIF3B · Spermiogenesis · Kinesin · Octopus · Testis

Introduction

Spermatogenesis is a highly ordered process, during which the spermatogenic stem cell develops into spermatozoa. After mitotic proliferation and meiotic division, spermiogenesis dramatically takes place with three subsequent significant events happening in spermatids: nucleus reshaping, acrosome biogenesis and flagellum formation [1, 2]. Contrary to our more substantial morphological knowledge about spermatogenesis, the functions of motor proteins during morphological rearrangements are still less understood. On account of the similarity in sperm structure morphological changes during spermiogenesis compared to mammals, we have used an octopod cephalopod *Octopus tankahkeei* as a suitable model system for the study of molecular mechanisms of spermatogenesis [3–7]. Kinesin II motor protein is typically a heterotrimeric complex composed of KIF3A/KIF3B or KIF3A/KIF3C heterodimers and

Ran Dang, Jun-Quan Zhu, and Fu-Qing Tan contributed equally to this work.

Electronic supplementary material The online version of this article (doi:10.1007/s11033-011-1363-4) contains supplementary material, which is available to authorized users.

R. Dang · J.-Q. Zhu · W. Wang
Faculty of Life Science and Bioengineering, Ningbo University, 315211 Zhejiang, People's Republic of China

R. Dang · W. Wang · H. Zhou · W.-X. Yang (✉)
The Sperm Laboratory, College of Life Sciences, Zhejiang University, Hangzhou 310058, People's Republic of China
e-mail: wxyang@spermlab.org

F.-Q. Tan
The First Affiliated Hospital, College of Medicine, Zhejiang University, Hangzhou 310003, People's Republic of China

a scaffold or adaptor non-motor protein KAP3 [8–15]. As originally found in the neuronal axon, KIF3 was used to drive fast anterograde transport, which is a microtubule plus-end directed activity pivotal for neurite elongation [10, 16–19] and neuronal polarity [20, 21]. There is also abundant evidence that KIF3 is responsible for transporting melanosomes and endosomes, the Golgi-ER secretary pathway, and also KIF3 takes part in mitosis [15, 22–25]. In addition, KIF3 is involved in Hedgehog signaling pathways on account of its contribution to the primary cilium, a specialized immotile cilium that has been implicated in intracellular signaling as the cell's antenna [26]. KIF3 also determines embryonic left–right asymmetry [27, 28]. Furthermore, KIF3 subunits are involved in intraflagellar transport (IFT), a bidirectional movement critical for the maintenance and assembly of motile cilia and flagella [29–33]. KIF3 function is particularly intriguing with respect to spermiogenesis because of the massive reorganization and development of both the axonemal tail and the specialized membrane components that occur during this process.

In a previous study, we found a homologue of rat C-terminal kinesin KIFC1 which participates in octopus sperm nucleus shaping via the microtubular structure manchette [34, 35]. We also isolated an N-terminal kinesin gene encoding a homologue of KIF3A which possibly takes part in intraflagellar and intramanchette transport in *O. tankahkeei* [36]. As we know, KIF3A and KIF3B always interact with each other, forming a stable heterodimer in intracellular transport. To date, nobody knows whether KIF3B participates in spermatogenesis as KIF3A does and its relationship with KIF3A during spermatogenesis in *O. tankahkeei*. Based on the observation of *kif3a* expression pattern and its association with *kif3b* [36], we hypothesize that the octopus homologue of *kif3b* shares a similar expression pattern with *ot-kif3a*, and the putative Kinesin II complex plays a key role in the flagellum elongation, intraflagellar transportation and intramanchette transportation.

For this paper, we cloned a cDNA encoding a highly conserved homologue of KIF3B for the first time and detected its distribution profile in various tissues of *O. tankahkeei*. In addition, we analyzed the expression pattern of *ot-kif3b* mRNA and compared it with the expression pattern of *ot-kif3a*, along with a corresponding discussion on the motor's potential functions during spermiogenesis in *O. tankahkeei*.

Materials and methods

Animals

Specimens of *O. tankahkeei* were purchased from Ningbo Aquatic Products Market from July, 2009 to November, 2010. Forty adult male individuals were selected, half of which were transported to the Sperm Laboratory at Zhejiang University in sea water tanks with aeration facility. Following temporary maintenance, the animals were anesthetized on ice and dissected to obtain the testis, heart, gill, muscle, stomach, liver and pancreas. The tissues were then swiftly placed and preserved in liquid nitrogen for RNA extraction. Testes and seminal vesicles from eight different animals were also subjected to fixation with 4% PFA-PBS (ph 7.4) for in situ hybridization. Meanwhile, the other twenty individuals were carried to the Faculty of Life Science and Bioengineering at Ningbo University and sampled in the same way for histological analysis and transmission electron microscopy, respectively.

RNA extraction and degenerate primer design

Total RNA was extracted following established protocols in our laboratory [34]. Protein sequences of KIF3B homologues from various species were aligned by Vector NTI advanced version.10 (Invitrogen) and a number of conserved blocks of amino acid residues were detected. Degenerate primers, F1, R1, R2 and F3 (Supplementary Table.S1) were designed using the online software CODEHOP (http://bioinformatics.weizmann.ac.il/blocks/codehop.html) based on the amino acid residues of selected regions.

cDNA synthesis and full-length *ot-kif3b* cDNA cloning

First-strand cDNA synthesis was conducted by HiFi-MMLV cDNA kit (CWBIO) according to the manufacture's instruction. Degenerate primers and a touchdown PCR strategy was used to obtain a cDNA fragment of *ot-kif3b*. The program was set as: 94°C for 180 s; 16 cycles of 94°C for 30 s, 55°C (which was reduced by 0.5°C each cycle) for 30 s and 72°C for 30 s; 20 cycles of 94°C for 30 s, 47°C for 30 s and 72°C for 40 s; 72°C for 10 min. Eventually, the PCR product was gel-excised, ligated to PMD-18T vector (Takara), transformed into DH5α Competent cells (Takara) and finally sequenced by Shanghai Sangon Company.

After a segment of the target cDNA was obtained, both 5′ and 3′ rapid-amplification of cDNA ends (RACE) were performed for the full-length *ot-kif3b* cDNA by utilizing Smart RACE cDNA amplification Kit (CloneTech) and 3′ Full RACE Amplification Kit (Takara) according to the Kit instructions. Gene specific primers (F4, F5, and R4) (Supplementary Table.S1) designed from the obtained sequence and adaptor primers supplied in the RACE Kit were used for the RACE-PCR reaction, of which the system and cycling conditions were recommended in the manual book. For the products purification, transformation and sequencing, see above.

Sequence analysis, multiple sequences alignment, and phylogenetic analysis

The sequence analysis of *ot-kif3b* cDNA and multiple sequences alignment was performed by the Vector NTI advanced version.10 (Invitrogen). Sequence comparison between *ot-kif3a* and *ot-kif3b* was operated by the BLAST program at the National Center for Biotechnology Information (http://blast.ncbi.nlm.nih.gov/). The phylogenetic analysis and statistical neighbor-joining bootstrap tests of the phylogenies were carried out by using the MEGA version 4.0 software. The secondary structure of ot-KIF3A and ot-KIF3B was predicted with Jpred 3 (http://www.compbio.dundee.ac.uk/www-jpred/).

Tissue expression pattern analysis

In order to examine tissue expression pattern of *ot-kif3b*, RNA extracted from the heart, gill, muscle, stomach, liver and pancreas of adult males underwent RT-PCR, respectively, with a pair of gene specific primers (TF and TR) (Supplementary Table.S1) resulting in a 233 bp product. PCR was running as follows: initial incubation at 94°C for 5 min; 30 cycles of 94°C for 30 s, 55°C for 30 s and 72°C for 30 s; 72°C for 10 min. Primers of octopus β-actin (Actin-F and Actin-R) were used as control.

Histological analysis

Samples for histological analysis were fixed in Bouin's fixative, and dehydrated in graded alcohols followed by infiltration with Histoclear (xylene) and paraffin. Then the samples were sectioned at 7 μm, stained with haematoxylin/eosin and observed under the light field of a Nikon Eclipse E80i fluorescence microscope.

Transmission electron microscopy

Ten samples for TEM were fixed in 2.5% glutaraldehyde (0.2 M sodium cacodylate buffer, pH 7.4) for 1–2 h at 4°C, then postfixed in 1% osmium tetroxide under the same condition. Samples were subsequently dehydrated and embedded in Spurr's resin. Thin sections were cut on a LKB-III ultramicrotome, double stained with uranium acetate and lead citrate, and then observed and photographed using a JEM-1200EX transmission electron microscope.

In situ hybridization

In situ hybridization was performed according to the methods used in our previous study [34]. Briefly, a 501 bp fragment of *ot-kif3b* was obtained by PCR using two gene specific primers (Probe-F1, Probe-R1) (Supplementary Table.S1) and ligated to PGEM-T EASY Vector (Promega). After that, DIG-11-UTP incorporated riboprobe complementary in a segment of *ot-kif3a* mRNA and was transcribed in vitro using related reagents and linearized plasmid as a template. Then sections from testes and seminal vesicle were prepared for the prehybridization and hybridization. The chromogenic reaction was performed using NBT and BCIP (Promega) after the sections were incubated with anti-DIG-Ap-conjugated Fab fragment (Roche Diagnostics). Finally the hybridized sections were observed under the bright field of a Nikon Eclipse E80i fluorescence microscope.

Results

Sequence analysis of *ot-kif3b* and comparison with *ot-kif3a*

The complete *ot-kif3b* cDNA (GenBank accession number HQ689699) (Supplementary Fig.S1.) we finally obtained consisted of a 102 bp 5′ untranslated region (UTR), a 2,208 bp open reading frame (ORF), and a 55 bp 3′ UTR. The ORF encoded a putative protein of 736 amino acids with a predicted molecular weight of 84 kDa and a theoretical isoelectric point of 8.75.

Alignment among predicted Ot-KIF3B and its homologues from vertebrates and invertebrates was shown in Supplementary Fig.S2. The result indicated that sequence of Ot-KIF3B shared 68, 68, 69, 68, and 67% identity with KIF3B from *Homo sapiens*, *Mus musculus*, *Gallus gallus*, *Danio rerio*, and *Xenopus laevis*, respectively. The putative ATP-binding domain including the VVVR CRP, NGTIFA, GQTGTGKT and DGENHIRVGKLNL VDLAGSERQ sequences and the microtubule-binding motif, HIPYRDSKLTRLL, were highly conserved among all the species. A phylogenic tree was constructed based on the amino acid sequences of KIF3B homologues from various organisms. The putative protein was closely related to KIF3B homologues from invertebrates to vertebrates (Supplementary Fig.S3.).

We previously reported a member of Kinesin II superfamily in *O. tankahkeei*, which was homologous to KIF3A and named Ot-KIF3A [36]. In order to elucidate the fundamental relationship between the two subunits, we compared their primary and secondary structures. A diagonal dot matrix comparison between Ot-KIF3A and Ot-KIF3B showed the regions of high identities (52% in overall length) expanding from the motor domain to the latter half of the stalk region (Fig. 1a). According to secondary structure prediction analysis, Ot-KIF3B has an NH_2-terminal motor domain, a coiled-coil stalk region and a COOH-terminal divergent tail domain (Fig. 1b).

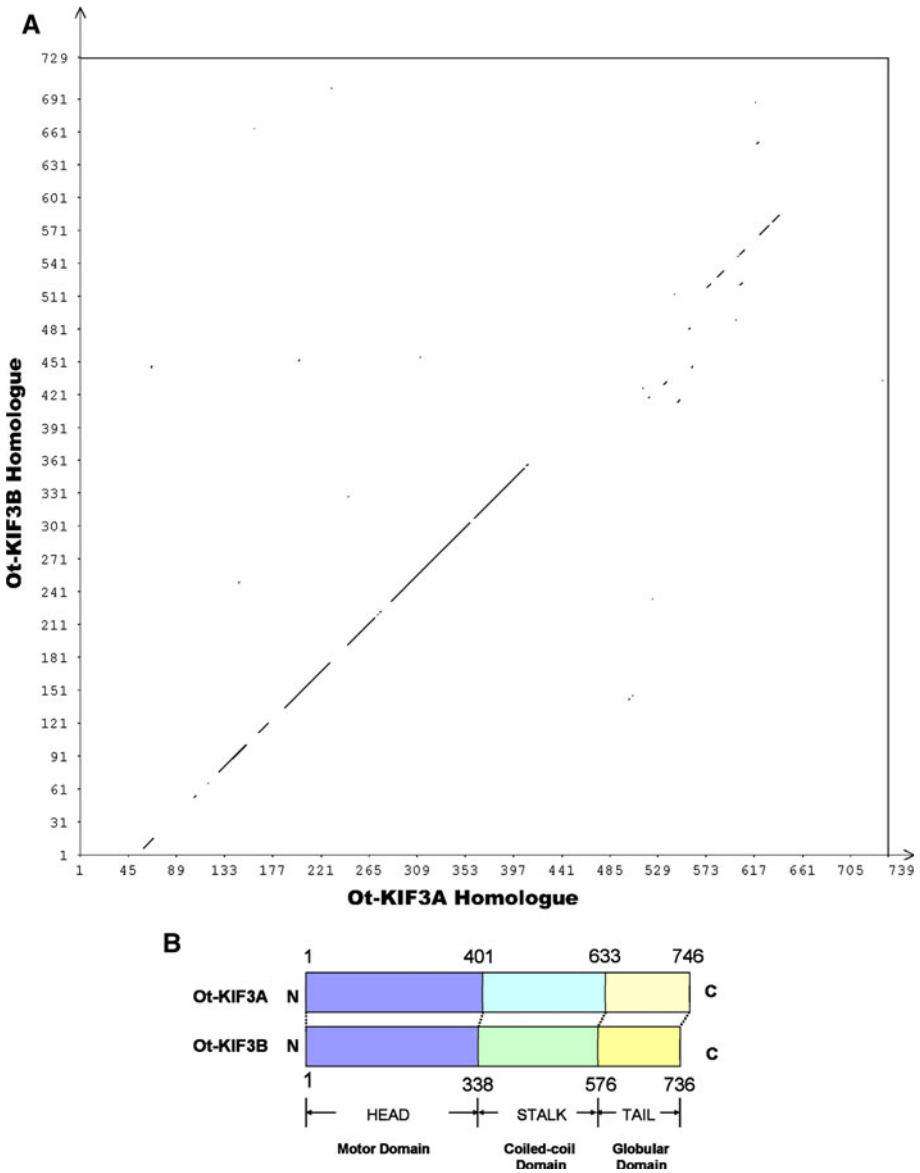

Fig. 1 Comparison of sequence and secondary structure of Ot-KIF3A and Ot-KIF3B. **a** Diagonal dot matrix view was performed for pairwise identities of Ot-KIF3A and Ot-KIF3B by Vector NTI advanced version.10 (Invitrogen) software using a window size of 8 and stringency of 60%. The Ot-KIF3A query sequence is represented on the *X*-axis and the numbers represent the bases/residues of the query. The Ot-KIF3B subject is represented on the *Y*-axis and again the numbers represent the bases/residues of the subject. Alignments are shown in the plot as *lines*. **b** Diagram showing the secondary structure predictions of Ot-KIF3A and Ot-KIF3B. Both contained an N-terminal highly conserved motor domain which may form a globular head, the coiled-coil stalk region, and a C-terminal tail region that was significantly different

Tissue distribution of *ot-kif3b*

To investigate the distribution pattern of *ot-kif3b* in different tissues from *O. tankahkeei*, RT-PCR with a pair of gene specific primer (TF1, TR1) (Supplementary Table.S1) were utilized to amplify a 233 bp cDNA fragment. The result showed that *ot-kif3b* was expressed in all the tissues above, but the expression level varies with different tissues (Fig. 2). Its expression was high in the gill, pancreas, and muscle, paralleled in the testis, heart and the stomach, and slightly lower in the liver.

Histological and morphogenesis changes in the testis and the spatial–temporal expression pattern of *ot-kif3b* during spermiogenesis

To explore the spatial and temporal expression pattern of *ot-kif3b* transcript during testis development and to determine the testicular cell types expressing this gene, we performed in situ hybridization and histological and transmission electron microscopy analysis. Our data showed that in early spermatid the nucleus was nearly round with mass-like chromatin condensed gradually.

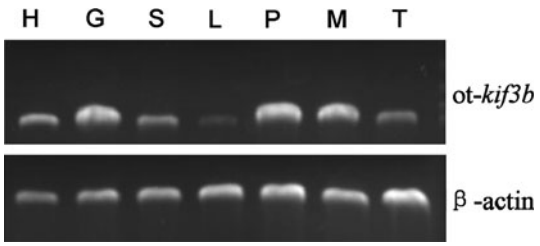

Fig. 2 The distribution of *ot-kif3b* by RT-PCR in various tissues of the *O. tankahkeei*. *β*-actin was used as a positive control (*lower panel*). *H* heart, *G* gill, *S* stomach, *L* liver, *P* pancreas, *M* muscle, *T* testis

Mitochondria were well-distributed in the cytoplasm near the Golgi apparatus (Fig. 3a, b). The mRNA signals were already detectable but weak in cytoplasm (Fig. 3c, d, arrow). As the flagellum emerged from the caudal end of the intermediate spermatid, the nucleus became eclipse-shaped and the chromatin existed as fibrosis. The posterior nuclear pocket invaginated deeply with the centriole located near the fossa of the pocket where axoneme of the tail originated (Fig. 3e, f). In this period, the message was expressed all over the cell and especially concentrated at the tail region (Fig. 3g, arrow). In late spermatid, the nucleus elongated into a long column and the chromatin compressed into stratification. It seemed clear that mitochondria aggregated to the posterior region of the spermatid (Fig. 3i, j). Obviously, the signal intensity increased to an extent reaching the maximum (Fig. 3h, k, arrow). Gradually, the *kif3b* transcripts accumulated around the nucleus and in the back of the spermatid, along with the growing tail (Fig. 3l). After the remodeled spermatid underwent significant morphological change, the final spermatid had a slim columned nucleus, with a highly condensed chromatin inside (Fig. 3m, n). In mature spermatozoa, the acrosomal vesicle became transferred into a helicoidal acrosomal cone (Fig. 3o), which was unique to the sperm of the octopod cephalopods [37]. The transcripts were abundant mostly around the nucleus and in the mid-piece of the tail (Fig. 3p, arrow). This expression pattern was in accordance with that of *ot-kif3a* during spermiogenesis of *O. tankahkeei* [36], suggesting they may maintain a close relationship in their functions. The general *ot-kif3a/b* expression pattern during spermiogenesis is illustrated using a schematic picture (Fig. 4).

Discussion

In eukaryotic cells, cytoskeleton, which forms a network, contributes to the cellular integrity. This network provides a highway for transporting and re-localizing of cellular components via the activity of molecular motors [38, 39]. Microtubule-dependent kinesin motors are essential for intracellular transport, carrying different cargoes, such as vesicles, membranous organelles, synthesized proteins, and mRNAs to specific destinations [40–44]. The developed delivery system determines the unique morphology and functions of differentiated cells, not only in neuron cells [43, 44] and somatic cells [45, 46] but also in germ cells [34–36, 47–50]. Kinesins have been demonstrated to play significant roles in spermiogenesis not only in mammals [51], but also in invertebrates [34–36, 50]. For instance, KIF2Aβ is distributed in the perinuclear area during spermatogenesis interacting with translin associated factor-X (TRAX) in mouse [51]. In intraflagellar transport (IFT), KIF17, interacting with the nuclear import protein (importin-β2), is proposed to be regulated by a ciliary localization signal (CLS) and inhibited by Ran GTPase to obtain a passport into the ciliary compartment [52]. A carboxyl-terminal (C-terminal) motor protein KIFC1 is believed to participate in a Golgi-acrosome bidirectional pathway and thus contribute to spermatid nuclear reshaping and acrosome morphogenesis in mammals [49, 53] as well as in crustaceans [50, 54]. However, the functions of kinesin motors during spermiogenesis in mollusks such as *Cephalopoda* remain unclear.

To date, the characterization of *kif3b* gene and its expression pattern during octopod spermiogenesis is reported in this work for the first time. The amino acids of Ot-KIF3B shared common features of the Kinesin II superfamily, including an amino-terminal motor domain, a coiled-coil stalk and a carboxy-terminal tail region. Multiple sequence alignments showed that sequences of the putative protein and KIF3B homologues from vertebrates were highly conserved in spite of the taxonomic distance between octopod and vertebrates, which is similar to the situation of Ot-KIF3A [36]. Based on the accepted argument that KIF3A and KIF3B always form a heterodimer at the α-helical rod domain, associating with the adaptor KAP3 [10, 12, 16, 18, 55], we compared the fundamental structures of Ot-KIF3A and Ot-KIF3B. Ot-KIF3B showed 53% identity in full length with Ot-KIF3A and they were extremely similar at the motor domain. Such identities suggested that the putative Ot-KIF3A and Ot-KIF3B may be alternative spliced variants of *kif3*.

Tissue distribution pattern of *ot-kif3b* revealed its ubiquitous expression in all the tissues examined at gene level was consistent with that of *ot-kif3a* [36]. This result was in agreement with reports proposing KIF3 was one of the most abundantly expressed KIFs, not only functioning in the best known intraflagellar transport but also in neural, melanosome, Golgi-ER transport, mitosis, and tumor suppression [12, 23, 24, 43]. We supposed that the function of this motor protein may not be restricted to testis, but was tissue specific relying on different microenvironments. In situ hybridization directly demonstrated that expression of *ot-kif3b* mRNA was gradually high throughout the developing spermatid. The expression profile of *ot-kif3b* was quite similar to that of *ot-kif3a*, but unlike *ot-kifc1* which was not expressed at mature stages [34].

Such extraordinary similarity of expression pattern between *ot-kif3a* and *ot-kfi3b*, together with the homologous fundamental structure, gave us strong reason to believe that the putative Ot-KIF3A and Ot-KIF3B may form a conventional heterodimeric complex, of which both coiled-coil stalks interacted stably with each other, just like in many vertebrates and invertebrates [10, 12, 13, 43].

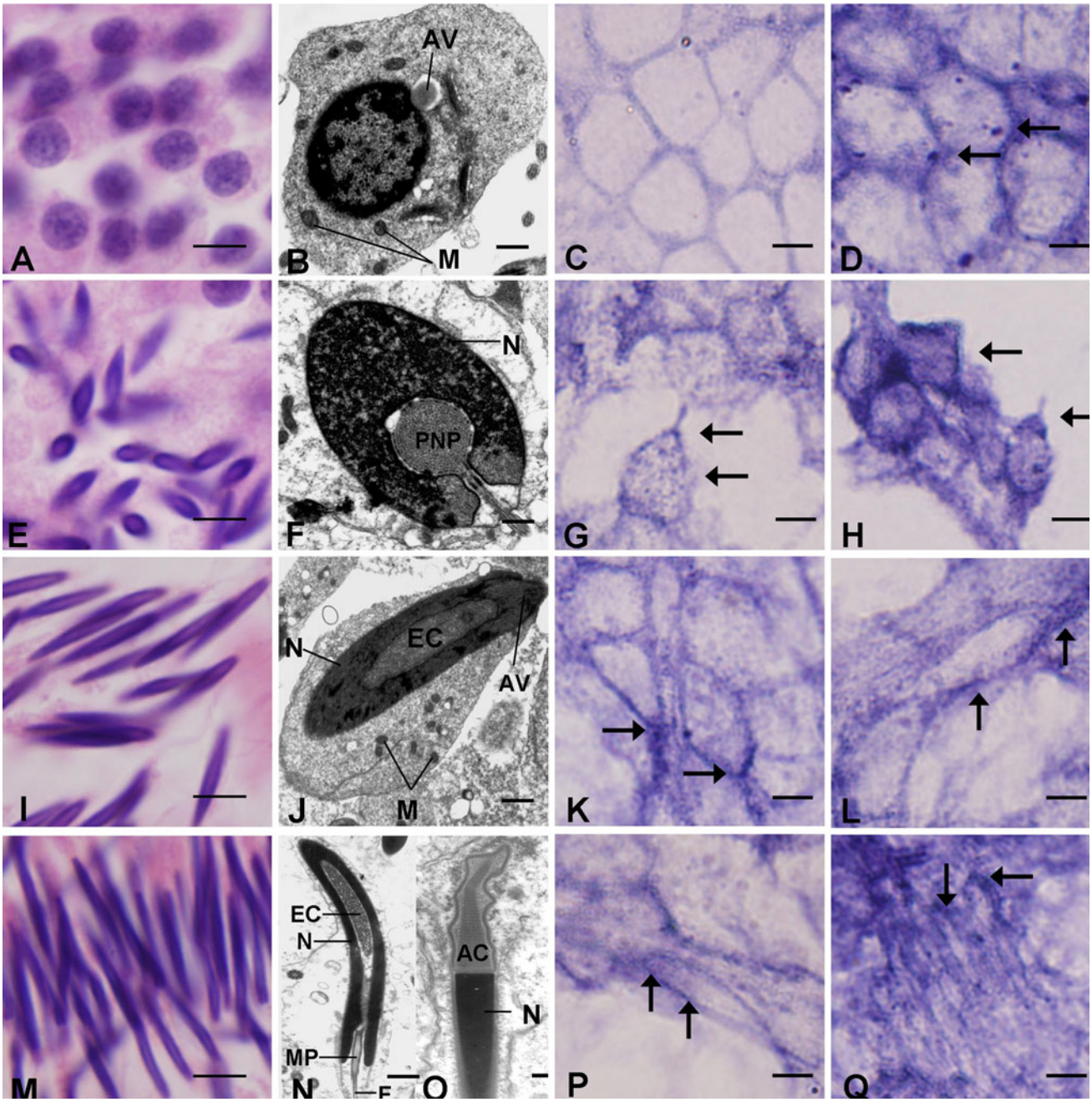

Fig. 3 Histological and morphogenesis changes in the testis and the spatial–temporal expression pattern of *ot-kif3b* during spermiogenesis. **a**, **b** In early spermatid, the nucleus was nearly round within mass like chromatin gradually condensed. The posterior of the nucleus depressed into a pocket while mitochondria were well-distributed in the cytoplasm near the Golgi apparatus. **c**, **d** In early spermatid, the signal is detected (*arrow*); **e**, **f** In intermediate spermatid, the nucleus shaped *ellipse* and the chromatin existed as fibrosis. The posterior nuclear pocket invaginated deeply. **g**, **h** The message expressed all over the cell, especially concentrating at the tail region (*arrow*). **i**, **j** In the late spermatid undergoing dramatic lateral compression and elongation, the acrosomal vesicle is long cystiform in shape at the apical tip while in the opposite part, endonuclear channel was formed. Mitochondria aggregated to the posterior region of the spermatid. **k**, **l** The message is abundant around the nuclear, enriching at the tail region (*arrow*). **m**–**o** The final spermatid had a slim columned nucleus in shape, with a highly condensed chromatin inside. The arosomal vesicle became into a helicoidal acrosomal cone. The flagellum is clear. **h** In final spermatid, the signal is mostly around the nucleus with the most intensity in the midpiece of the tail (*arrow*). **q** In mature sperm, the expression pattern is similar to that of the final spermatid (*arrow*). **a**, **e**, **i**, **m**, histological analysis, by HE staining. Scale bar, 2 μm; **b**, **f**, **j**, **n**, **o** Transmission Electron Microscopy analysis. *Scale bar*, 0.5 μm. **c**, **d**, **g**, **h**, **k**, **l**, **p**, **q** in situ hybridization analysis. *Arrows* indicated *ot-kif3b* transcripts in corresponding stages. *Scale bar*, 1 μm. *AV* acrosomal vesicle, *M* mitochondria, *N* nucleus, *PNP* posterior nuclear pocket, *EC* endonuclear channel, *MP* midpiece, *F* flagellum, *AC* acrosomal cone

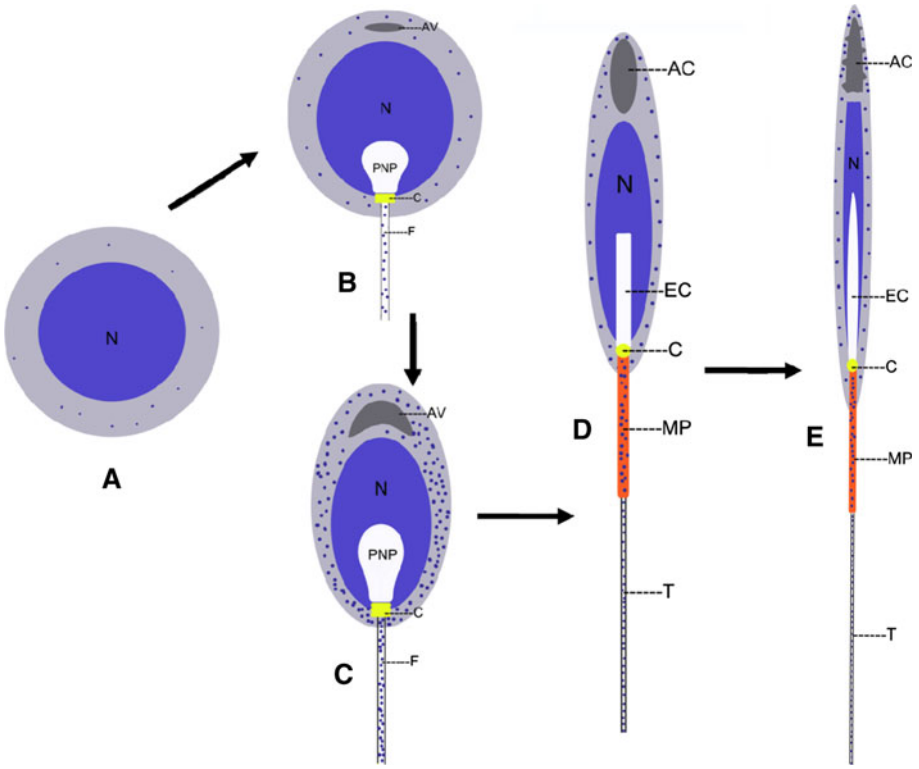

Fig. 4 A schematic model produced on the basis of the previous exhibition and representing the spatial and temporal expression profile of *ot-kif3b* during spermiogenesis of *O. tankahkeei.* The *blue* spherical granule indicates the mRNA transcripts with a corresponding density. **a** In early spermatid, the signal is already appeared with a low level. **b** In intermediate spermatid, the transcripts gradually increase as well as emerge in the growing tail. **c** In drastically remodeling spermatid, the messages distribute along the longitudinal elongation and get the maximum. **d** In late spermatid, the signal is still abundant especially around the nucleus and in the midpiece and the tail. **e** In mature spermatid, the transcripts are still visible. *N* nucleus, *AV* acrosomal vesicle, *PNP* posterior nuclear pocket, *C* centrioles, *F* flagellum, *AC* acrosomal cone. *EC* endonuclear channel, *MP* midpiece, *T* tail

From intermediate to mature spermatids, the expression of *ot-kif3a/b* is abundant in the midpiece and flagellum of the tail. These observations agree with a previous study claiming that the heterodimeric kinesin II is associated with the midpiece and flagellum of spermatic cells in sea urchins [56] and rats [38]. Further studies proposed that the complex was essentially involved in intraflagellar transport (IFT) [30, 57]. Kinesin II transports the rafts along microtubules to the tip of the axoneme beneath the flagellum membrane [30, 57–59]. Considering IFT transport is evolutionarily conserved [29] and the striking similar structure of the sperm flagella between *O. tankahkeei* and mammals, we assume that Ot-KIF3B with its close partner Ot-KIF3A, may take part in the maintenance and assembly of the sperm flagellar axoneme.

Sharing a similar molecular mechanism to IFT, intramanchette transport (IMT) also requires Kinesin II hetero dimeric homoenzyme [60]. In *O. tankahkeei*, a microtubule-based perinuclear structure was observed transiently during spermiogenesis [4, 35], which was in agreement with another cephalopod, *S. officinalis* possessing the same structure originating from the spermatid head [61]. Since the perinuclear structure plays the same as mammalian manchette [4, 35], the abundant distribution of *ot-kif3a/b* around the perinulear structure shed light on the potential function of this proteins in IMT transport. Likewise, Ot-KIFC1 was co-localized with the manchette-like structure, which was proved to participate in sperm nuclear morphogenesis as its homologue does in rodents [35, 49]. Based on the findings above, however, we are still not sure whether Ot-KIF3A/B takes part in sperm nuclear reshaping through bridging the manchette-like perinuclear microtubules in association with Ot-KIFC1. Even if they did, they must have a distinct mechanism for processes depending on their reverse direction of transportation.

In *O. tankahkeei*, mitochondria are actively transported posteriorly and eventually form the chondriosomal mantle at mid-piece of the spermatid in biological adaption to internal fertilization. During spermiogenesis, IMT and IFT deliver cargoes for the tail formation, prompting that mitochondria may aggregate in the mid-piece by IMT and IFT [62]. Interestingly, the *ot-kif3a/b* transcripts expression profile was consistent with the dynamics of mitochondria, making it plausible to speculate the relationship between mitochondria and KIF3A/B in spermatid tail development. In a sense, this

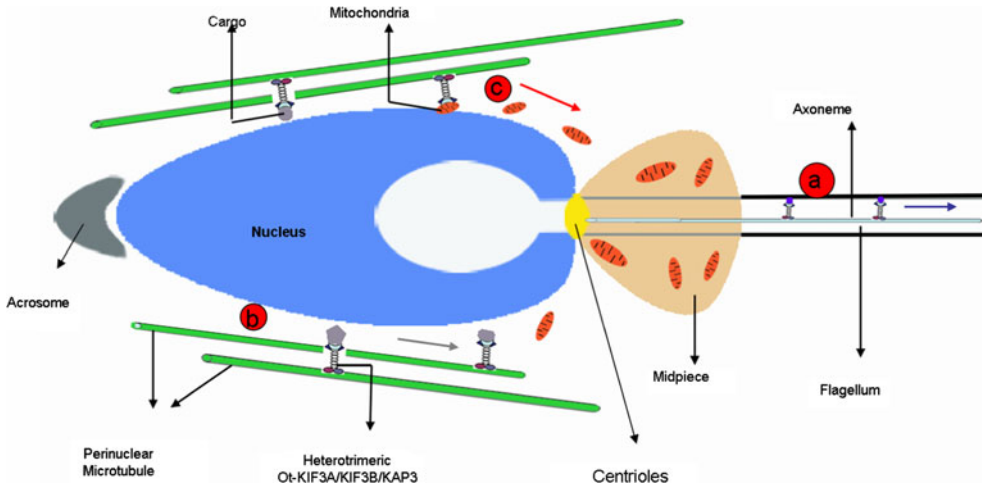

Fig. 5 A schematic model displaying the three possible functions of the putative Ot-KIF3A/B heterodimer during spermiogenesis of *O. tankahkeei*. **a** The complex drive different IFT particles to which the scaffolding/adaptor protein KAP3 directly linking, from the distal to the tip of the axon beneath the flagellum membrane, involving in the formation of flagellum and primary cilia, further accomplishing some signaling transduction pathway. **b** Along the manchette-like perinulear microtubules, Kinesin II may carry some IMT rafts and further operating the nucleocytoplasmic exchange activities. **c** The heterodimer may in a sense contribute to the aggregation of mitochondria in the midpiece

assumption supplements a previous suggestion that only KIF1Bα, which belongs to the kinesin 3 family, and KIF5 motors play roles in mitochondrial transport [43, 62, 63]. However, the information available at present doesn't allow a thorough investigation of the distribution of mitochondria during spermiogenesis of *O. tankahkeei.* Further studies on the localization of KIF3A/B and mitochondria as well as the machinery between motor proteins and corresponding adaptors will be required before the hypothesis can be advanced to a conclusion regarding the specific transport role in this process [63–65].

Moreover, the timing and synchrony of spermatid differentiation need signaling transduction between spermatogenic cells and between Sertoli cells and Leydig cells [66, 67], which is possibly achieved through participation of the cell's sensory organelle, or primary cilia. It is recommended that through IFT, primary cilium works as eukaryotic cell's antenna transducing a multitude of sensory stimuli to coordinate a number of physiological and developmental signaling pathways [58, 68, 69]. Because of its involvement in intraflagellar transport, KIF3 is also implicated in some signaling pathways such as Hedgehog and Wnt pathways [26, 70]. Since *ot-kif3a/b* transcripts were enriched at the tail region at late and final stages, it's likely that Ot-KIF3A/B may help the coordination among different cells in testis via regulating the behavior of primary cilia or some signaling factors. Nonetheless, more experiments with direct protein function analysis are still required to ascertain the function of Ot-KIF3A/B.

In conclusion, our results revealed that the octopus homologue of KIF3B firstly detected is in high identities with Ot-KIF3A, reported before by our laboratory, in fundamental structures and shares a similar expression pattern with *ot-kif3a*, all of which support our hypothesis on their potential interactions in intraspermatid transport during spermiogenesis of *O. tankahkeei*. The putative heterodimer may be involved in intraflagellar and intramanchette transport by carrying different cargoes to a specific destination, hereby playing key roles in the formation of flagellum and primary cilia. This protein complex may also participate in some signaling transduction pathway and operate the nucleocytoplasmic exchange activities. Furthermore, the heterodimer may in a sense contribute to the aggregation of mitochondria to the midpiece. A schematic model about possible functions of the putative Ot-KIF3A/B heterodimer during spermiogenesis of *O. tankahkeei* is displayed on Fig. 5.

Acknowledgments We would like to thank all the members of the Sperm Laboratory at Zhejiang University. We are also grateful to Mr. Jia-Qiang Yan and other members in Professor Zhu Jun-Quan's laboratory at Ningbo University for materials preparation. This project was supported in part by: (1) Zhejiang Provincial Natural Science Foundation of China (Grant No Z307536 and Y2100296); (2) National Natural Science Foundation of China, Grant number: No. 31072198 and 40776079; (3) K. C. Wong Magna Fund in Ningbo University; (4) the Scientific Research Foundation of Graduate School of Ningbo University (Grant No NG09JLA013).

References

1. Fawcett DW (1975) The mammalian spermatozoon. Dev Biol 44:394–436
2. Wang R, Sperry AO (2008) Identification of a novel leucine-rich repeat protein and candidate PP1 regulatory subunit expressed in developing spermatids. BMC Cell Biol 9:9

3. Zhu JQ, Yang WX, You ZJ, Jiao HF (2005) The ultrastructure of the spermatozoon of *Octopus tankahkeei*. J Shellfish Res 24:1203–1207
4. Zhu JQ, Yang WX, You ZJ, Wang W, Jiao HF (2006) Ultrastructure of spermatogenesis of *Octopus tankahkeei*. J Fish China 30:161–169
5. Jiao HF, You ZJ, Wang YN (2008) Study on the foundational biological character of *Octopus tankahkeei*. Acta Oceanol Sinica 5:90–95
6. Li Z, Zhu JQ, Yang WX (2010) Acrosome reaction in *Octopus tankahkeei* induced by calcium ionophore A23187 and a possible role of the acrosomal screw. Micron 41:39–46
7. Yu HM, Wang W, Zhu JQ, Yang WX (2010) Analysis on dynamic distribution and function of microtubule during *Octopus tankahkeei* spermiogenesis. Chin Cell Biol 32:251–255
8. Berezuk MA, Schroer TA (2004) Fractionation and characterization of kinesin II species in vertebrate brain. Traffic 5: 503–513
9. Hirokawa N (1998) Kinesin and dynein superfamily proteins and the mechanism of organelle transport. Science 279:519–526
10. Hirokawa N (2000) Stirring up development with the heterotrimeric kinesin KIF3. Traffic 1:29–34
11. Lawrence CJ, Dawe RK, Christie KR, Cleveland DW, Dawson SC, Endow SA, Goldstein LS, Goodson HV, Hirokawa N, Howard J, Malmberg RL, McIntosh JR, Miki H, Mitchison TJ, Okada Y, Reddy AS, Saxton WM, Schliwa M, Scholey JM, Vale RD, Walczak CE, Wordeman L (2004) A standardized kinesin nomenclature. J Cell Biol 167:19–22
12. Marszalek JR, Goldstein LS (2000) Understanding the functions of kinesin-II. Biochim Biophys Acta 1496:142–150
13. Miki H, Okada Y, Hirokawa N (2005) Analysis of the kinesin superfamily: insights into structure and function. Trends Cell Biol 15:467–476
14. Miki H, Setou M, Kaneshiro K, Hirokawa N (2001) All kinesin superfamily protein, KIF, genes in mouse and human. Proc Natl Acad Sci USA 98:7004–7011
15. Navone F, Consalez GG, Sardella M, Caspani E, Pozzoli O, Frassoni C, Morlacchi E, Sitia R, Sprocati T, Cabibbo A (2001) Expression of KIF3C kinesin during neural development and in vitro neuronal differentiation. J Neurochem 77:741–753
16. Aizawa H, Sekine Y, Takemura R, Zhang Z, Nangaku M, Hirokawa N (1992) Kinesin family in murine central nervous system. J Cell Biol 119:1287–1296
17. Cole DG, Chinn SW, Wedaman KP, Hall K, Vuong T, Scholey JM (1993) Novel heterotrimeric kinesin-related protein purified from sea urchin eggs. Nature 366:268–270
18. Yamazaki H, Nakata T, Okada Y, Hirokawa N (1995) KIF3A/B: a heterodimeric kinesin superfamily protein that works as a microtubule plus end-directed motor for membrane organelle transport. J Cell Biol 130:1387–1399
19. Wedaman KP, Meyer DW, Rashid DJ, Cole DG, Scholey JM (1996) Sequence and submolecular localization of the 115-kD accessory subunit of the heterotrimeric kinesin-II (KRP85/95) complex. J Cell Biol 132:371–380
20. Nishimura T, Kato K, Yamaguchi T, Fukata Y, Ohno S, Kaibuchi K (2004) Role of the PAR-3-KIF3 complex in the establishment of neuronal polarity. Nat Cell Biol 6:328–334
21. Shi SH, Cheng T, Jan LY, Jan YN (2004) APC and GSK-3β are involved in mPar3 targeting to the nascent axon and establishment of neuronal polarity. Curr Biol 14:2025–2032
22. Brown CL, Maier KC, Stauber T, Ginkel LM, Wordeman L, Vernos I, Schroer TA (2005) Kinesin-2 is a motor for late endosomes and lysosomes. Traffic 6:1114–1124
23. Haraguchi K, Hayashi T, Jimbo T, Yamamoto T, Akiyama T (2006) Role of the kinesin-2 family protein, KIF3, during mitosis. J Biol Chem 281:4094–4099
24. Stauber T, Simpson JC, Pepperkok R, Vernos I (2006) A role for kinesin-2 in COPI-dependent recycling between the ER and the Golgi complex. Curr Biol 16:2245–2251
25. Schonteich E, Wilson GM, Burden J, Hopkins CR, Anderson K, Goldenring JR, Prekeris R (2008) The Rip11/Rab11-FIP5 and kinesin II complex regulates endocytic protein recycling. J Cell Sci 121:3824–3833
26. Ocbina PJ, Anderson KV (2008) Intraflagellar transport, cilia, and mammalian Hedgehog signaling: analysis in mouse embryonic fibroblasts. Dev Dyn 37:2030–2038
27. Nonaka S, Tanaka Y, Okada Y, Takeda S, Harada A, Kanai Y, Kido M, Hirokawa N (1998) Randomization of left-right asymmetry due to loss of nodal cilia generating leftward flow of extraembryonic fluid in mice lacking KIF3B motor protein. Cell 95:829–837
28. Hirokawa N, Tanaka Y, Okada Y, Takeda S (2006) Nodal flow and the generation of left-right asymmetry. Cell 125:33–45
29. Baker SA, Freeman K, Luby-Phelps K, Pazour GJ, Besharse JC (2003) IFT20 links kinesin II with a mammalian intraflagellar transport complex that is conserved in motile flagella and sensory cilia. J Biol Chem 278:34211–34218
30. Ou G, Blacque OE, Snow JJ, Leroux MR, Scholey JM (2005) Functional coordination of intraflagellar transport motors. Nature 436:583–587
31. Pan X, Ou G, Civelekoglu-Scholey G, Blacque OE, Endres NF, Tao L, Mogilner A, Leroux MR, Vale RD, Scholey JM (2006) Mechanism of transport of IFT particles in *C. elegans* cilia by the concerted action of kinesin-II and OSM-3 motors. J Cell Biol 174:1035–1045
32. Scholey JM (2008) Intraflagellar transport motors in cilia: moving along the cell's antenna. J Cell Biol 180:23–29
33. Serra R (2008) Role of intraflagellar transport and primary cilia in skeletal development. Anat Rec (Hoboken) 291:1049–1061
34. Wang W, Zhu JQ, Yang WX (2010) Molecular cloning and characterization of KIFC1-like kinesin gene (*ot-kifc1*) from *Octopus tankahkeei*. Comp Biochem Physiol B Biochem Mol Biol 156:174–182
35. Wang W, Zhu JQ, Yu HM, Tan FQ, Yang WX (2010) KIFC1-like motor protein associates with the cephalopod manchette and participates in sperm nuclear morphogenesis in *Octopus tankahkeei*. Plos One 5:1–11
36. Wang W, Dang R, Zhu JQ, Yang WX (2010) Identification and dynamic transcription of KIF3A homologue gene in spermiogenesis of *Octopus tankahkeei*. Comp Biochem Physiol A Mol Integr Physiol 157:237–245
37. Franzén A (1967) Spermiogenesis and spermatozoa of the Cephalopoda. Ark Zool 19:323–334
38. Miller MG, Mulholland DJ, Vogl AW (1999) Rat testis motor proteins associated with spermatid translocation (dynein) and spermatid flagella (kinesin-II). Biol Reprod 60:1047–1056
39. Navolanic PM, Sperry AO (2000) Identification of isoforms of a mitotic motor in mammalian spermatogenesis. Biol Reprod 62: 1360–1369
40. Vale RD (2003) The molecular motor toolbox for intracellular transport. Cell 112:467–480
41. Hirokawa N, Takemura R (2004) Kinesin superfamily proteins and their various functions and dynamics. Exp Cell Res 301: 50–59
42. Seog DH, Lee DH, Lee SK (2004) Molecular motor proteins of the kinesin superfamily proteins (KIFs): structure, cargo and disease. J Korean Med Sci 19:1–7
43. Hirokawa N, Noda Y, Tanaka Y, Niwa S (2009) Kinesin superfamily motor proteins and intracellular transport. Natl Rev Mol Cell Biol 10:682–696
44. Verhey KJ, Hammond JW (2009) Traffic control: regulation of kinesin motors. Natl Rev Mol Cell Biol 10:765–777

45. Noda Y, Okada Y, Saito N, Setou M, Xu Y, Zhang Z, Hirokawa N (2001) KIFC3, a microtubule minus end-directed motor for the apical transport of annexin XIIIb-associated Triton-insoluble membranes. J Cell Biol 155:77–88
46. Bernasconi P, Cappelletti C, Navone F, Nessi V, Baggi F, Vernos I, Romaggi S, Confalonieri P, Mora M, Morandi L, Mantegazza R (2008) The kinesin superfamily motor protein KIF4 is associated with immune cell activation in idiopathic inflammatory myopathies. J Neuropathol Exp Neurol 67:624–632
47. Sperry AO, Zhao LP (1996) Kinesin-related proteins in the mammalian testes: candidate motors for meiosis and morphogenesis. Mol Biol Cell 7:289–305
48. Zou Y, Millette CF, Sperry AO (2002) KRP3A and KRP3B: candidate motors in spermatid maturation in the seminiferous epithelium. Biol Reprod 66:843–855
49. Yang WX, Sperry AO (2003) C-Terminal kinesin motor KIFC1 participates in acrosome biogenesis and vesicle transport. Biol Reprod 69:1719–1729
50. Wang DH, Yang WX (2010) Molecular cloning and characterization of KIFC1-like kinesin gene (es-KIFC1) in the testis of the Chinese mitten crab *Eriocheir sinensis*. Comp Biochem Physiol A Mol Integr Physiol 157:123–131
51. Bray JD, Chennathukuzhi VM, Hecht NB (2004) KIF2Aβ: a kinesin family member enriched in mouse male germ cells, interacts with translin associated factor-X (TRAX). Mol Reprod Dev 69:387–396
52. Dishinger JF, Kee HL, Jenkins PM, Fan S, Hurd TW, Hammond JW, Truong YN, Margolis B, Martens JR, Verhey KJ (2010) Ciliary entry of the kinesin-2 motor KIF17 is regulated by importin-B2 and RanGTP. Nat Cell Biol 12:703–710
53. Yang WX, Jefferson H, Sperry AO (2006) The molecular motor KIFC1 associates with a complex containing nucleoporin NUP62 that is regulated during development and by the small GTPase RAN. Biol Reprod 74:684–690
54. Yu KM, Hou L, Zhu JQ, Ying XP, Yang WX (2009) KIFC1 participates in acrosomal biogenesis, with discussion of its importance for the perforatorium in the Chinese mitten crab *Eriocheir sinensis*. Cell Tissue Res 337:113–123
55. Kondo S, Sato-Yoshitake R, Noda Y, Aizawa H, Nakata T, Matsuura Y, Hirokawa N (1994) KIF3A is a new microtubule-based anterograde motor in the nerve axon. J Cell Biol 125:1095–1107
56. Henson JH, Cole DG, Roesener CD, Capuano S, Mendola RJ, Scholey JM (1997) The heterotrimeric motor protein kinesin-II localizes to the midpiece and flagellum of sea urchin and sand dollar sperm. Cell Motil Cytoskelet 38:29–37
57. Cole DG, Diener DR, Himelblau AL, Beech PL, Fuster JC, Rosenbaum JL (1998) Chlamydomonas kinesin-II-dependent intraflagellar transport (IFT): IFT particles contain proteins required for ciliary assembly in *Caenorhabditis elegans* sensory neurons. J Cell Biol 141:993–1008
58. Singla V, Reiter JF (2006) The primary cilium as the cell's antenna: signaling at a sensory organelle. Science 313(5787): 629–633
59. Scholey JM (2003) Intraflagellar transport. Annu Rev Cell Dev Biol 19:423–443
60. Kierszenbaum AL (2002) Intramanchette transport (IMT): managing the making of the spermatid head, centrosome and tail. Mol Reprod Dev 63:1–4
61. Martínez-Soler F, Kurtz K, Chiva M (2007) Sperm nucleomorphogenesis in the cephalopod *Sepia officinalis*. Tissue Cell 39:99–108
62. Sun X, Yang WX (2010) Mitochondria: transportation, distribution and function during spermiogenesis. Adv Biosci Biotechnol 1:97–109
63. Cho KI, Cai Y, Yi H, Yeh A, Aslanukov A, Ferreira PA (2007) Association of the kinesin-binding domain of RanBP2 to KIF5B and KIF5C determines mitochondria localization and function. Traffic 8:1722–1735
64. Cai Q, Gerwin C, Sheng ZH (2005) Syntabulin-mediated anterograde transport of mitochondria along neuronal processes. J Cell Biol 170:959–969
65. Glater EE, Megeath LJ, Stowers RS, Schwarz TL (2006) Axonal transport of mitochondria requires milton to recruit kinesin heavy chain and is light chain independent. J Cell Biol 173:545–557
66. Mruk DD, Cheng CY (2004) Sertoli–Sertoli and Sertoli-germ cell interactions and their significance in germ cell movement in the seminiferous epithelium during spermatogenesis. Endocr Rev 25:747–806
67. Ruwanpura SM, McLachlan RI, Meachem SJ (2010) Hormonal regulation of male germ cell development. J Endocrinol 205: 117–131
68. Marshall WF, Nonaka S (2006) Cilia: tuning into the cell's antenna. Curr Biol 16(15):604–614
69. Pedersen LB, Rosenbaum JL (2008) Intraflagellar transport (IFT) role in ciliary assembly, resorption and signaling. Curr Top Dev Biol 85:23–61
70. Corbit KC, Shyer AE, Dowdle WE, Gaulden J, Singla V, Chen MH, Reiter JF (2008) Kif3a constrains β-catenin-dependent Wnt signalling through dual ciliary and non-ciliary mechanisms. Nat Cell Biol 10(1):70–76